Available online at www.sciencedirect.com
SCIENCE DIRECT®
Biochimica et Biophysica Acta 1611 (2003) 44–54
BIOCHIMICA ET BIOPHYSICA ACTA
BBA
www.bba-direct.com

Effect of polylysine on transformations and permeability of negative vesicular membranes

A.A. Yaroslavov[a,*], O.Ye. Kuchenkova[a], I.B. Okuneva[a], N.S. Melik-Nubarov[a], N.O. Kozlova[a], V.I. Lobyshev[b], F.M. Menger[c], V.A. Kabanov[a]

[a] School of Chemistry, M.V. Lomonosov Moscow State University, Leninskie Gory, Moscow 119899, Russian Federation
[b] School of Physics, M.V. Lomonosov Moscow State University, Leninskie Gory, Moscow 119899, Russian Federation
[c] Department of Chemistry, Emory University, Atlanta, GA 30322, USA

Received 7 May 2002; received in revised form 22 November 2002; accepted 13 December 2002

Abstract

Small (40–60 nm in diameter) and large (300–350 nm) negative vesicles were complexed with a cationic polypeptide, poly-L-lysine (PL). Laser microelectrophoresis experiments showed that in small vesicles rendered anionic with the addition of cardiolipin (CL^{2-}), only the CL^{2-} in the outer leaflet is involved in the complexation with PL. Calorimetric and other data demonstrate that the binding of PL to the membrane surface causes domains ("rafts") of CL^{2-} to form in the outer leaflet, and it is these domains that electrostatically bind the polymer. The kinetics of transmembrane permeation of doxorubicin (Dox, a fluorescent anti-tumor drug) was monitored with and without PL binding to the outer surface of the vesicles. It was found that PL mediates the permeation of Dox into the vesicle interior. In the absence of PL, the Dox molecule (possessing an amino group of pK_a=8.6) binds to the anionic vesicles in the protonated form and, consequently, suffers an impaired mobility through the membrane. On the other hand, when the PL covers the vesicle surface, Dox passes though the membrane with greater ease. The effects of salt and polyanion on the stability of PL–vesicle complexes and the PL-mediated Dox permeation are also discussed.

Keywords: Lipid vesicle; Polylysine; Doxorubicin; Lateral segregation; Membrane permeability

1. Introduction

The interaction of native and synthetic polyelectrolytes with biological and artificial lipid membranes has been intensively studied for the last 30 years, being stimulated by permanently growing biomedical applications of such polymers. In particular, polycations were found to increase the permeability of cell membranes towards antibacterial drugs [1] as well as oligonucleotides and DNA molecules [2–6] that allowed to control cell functioning. At the same time, it was shown that binding of cationic derivatives of poly(4-vinylpyridine) to negative lipid bilayer vesicles, whose membranes were in the fluid state (liquid vesicles), caused a migration of anionic lipids from the inner to outer membrane leaflet (polycation-induced flip-flop) [7]. The membrane retained their integrity unless the molar fraction of anionic lipid, v, exceeded 0.3. At higher v values, the polycation binding resulted in irreversible membrane disruption [8]. The protein–lipid membranes of living cells are in the fluid state as well, the fraction of anionic lipids being rather high [9]. It seems likely therefore that adsorption of polycations on the cell surface could also induce flip-flop of anionic lipids, finally resulting in destruction of cells. If so, an ability of polycations to accelerate the transmembrane migration of lipid molecules becomes an undesirable factor, restricting their biomedical application.

In the present work, small (40–60 nm in diameter) and large (300–350 nm in diameter) negative lipid vesicles were

Abbreviations: EL, egg yolk lecithin; DPPC, dipalmitoylphosphatidylcholine; CL^{2-}, diphosphatidylglycerol (cardiolipin); PC-pyrene, β-(pyrene-1-yl)decanoyl-γ-palmitoylphosphatidylcholine; FITC, *N*-fluorescein-*iso*-thiocyanate; PL, poly-L-lysine; PAA, polyacrylic acid; Dox, doxorubicin; DP, degree of polymerization; SUVs, small unilamellar vesicles; LUVs, large unilamellar vesicles; v, molar content of negative CL^{2-} headgroups in the vesicles; D, mean hydrodynamic diameter; EPM, electrophoretic mobility; DSC, differential scanning calorimetry; k_p and k_0, rate constants for transmembrane doxorubicin (Dox) permeation in the presence and in the absence of PL, respectively; $Z_{+/-}$, ratio between the number of positive PL units bound to vesicles and the total number of CL^{2-} headgroups in the system

* Corresponding author. Tel.: +7-095-939-3114; fax: +7-095-939-0174.
E-mail address: yaroslav@genebee.msu.su. (A.A. Yaroslavov).

0005-2736/02/$ - see front matter © 2002 Published by Elsevier Science B.V.
doi:10.1016/S0005-2736(02)00701-0

complexed with a synthetic cationic polypeptide, poly-L-lysine (PL). This cationic polypeptide was reported to strongly adsorb on the membrane of negative vesicles [10–13], enabling permeation of DNA through cell membranes [3,4]. However, it is not known if PL adsorption is able to induce flip-flop of lipid molecules and can affect the membrane permeability towards bioactive compounds. The following items were investigated:

(1) the structural rearrangements in the vesicular membrane induced by PL adsorption;
(2) the composition of PL–vesicle complexes;
(3) the stability of PL–vesicle complexes in water–salt solutions and in the presence of a competing polyanion; and
(4) the effect of adsorbed PL on transmembrane permeation of antitumor Dox.

2. Experimental

2.1. Materials

PL hydrobromide with degree of polymerization (DP) equal to 430, PL hydrobromide covalently modified by *N*-fluorescein-*iso*-thiocyanate (PL-FITC) with DP=250, egg yolk lecithin (EL), dipalmitoylphosphatidylcholine (DPPC), diphosphatidylglycerol (cardiolipin, CL^{2-}), β-(pyrene-1-yl)decanoyl-γ-palmitoylphosphatidylcholine (PC-pyrene), and Dox from Sigma, USA, and polyacrylic acid (PAA) with DP=70 from Aldrich, USA were used as received.

Fluorescently labeled PAA was prepared as follows: 20 mg of *N*-fluorescein-*iso*-thiocyanate (FITC) and 60 mg of 1,6-hexanediamine (both from Sigma) were dissolved in a mixture of 1 ml of dimethylformamide (DMF) and 0.2 ml of 0.1 M sodium carbonate buffer with pH 9.0. After incubation for 6 h in the dark at room temperature, the reaction mixture was fractionated by thin-layer chromatography on Silufol silica gel plates (Avalier, Czech Republic) using an ethanol/water/acetic acid (1:1:0.05) eluent system, which yielded 15 mg of NH_2-containing FITC. The latter was dissolved in 2 ml of DMF and mixed with water solution of PAA (50 mg/10 ml) in the presence of water soluble *N*-ethyl-*N*′-diethylaminopropyl carbodiimide (Sigma) following the procedure described in Ref. [14]. Upon completing the reaction, the excess of NH_2-containing FITC was separated by dialysis against 0.2 M sodium chloride solution and then against distilled water. Concentration of carboxylic group in the dialyzed solution was determined by pH titration, the content of FITC residues was estimated spectrophotometrically taking extinction coefficient equal to 80,000 M^{-1} cm^{-1}. Thus prepared FITC-attached PAA (PAA-FITC) was found to contain 1 FITC residue per 105 acrylate units.

To prepare EL/CL^{2-} and DPPC/CL^{2-} small unilamellar vesicles (SUVs) with diameter 40–60 nm, we followed the sonication procedure described in Ref. [15]. EL/CL^{2-} large unilamellar vesicles (LUVs) with diameter 300–400 nm were prepared according to the reverse-phase evaporation procedure [16]. The molar content of negative CL^{2-} headgroups in the vesicles, v, was specified as $v=2[CL^{2-}]/(2[CL^{2-}]+[EL])=2[CL^{2-}]/(2[CL^{2-}]+[DPPC])$ (each CL^{2-} molecules carries two anionic headgroups).

EL/CL^{2-} SUVs and LUVs with PC-pyrene incorporated into the bilayer were prepared as described above; 0.5 wt.% of PC-pyrene was added to the lipid mixture.

2.2. Methods

The mean hydrodynamic diameter (D) of vesicles and their complexes with polyelectrolytes was determined by photon correlation spectroscopy in a thermostatic cell with a fixed 90° scattering angle using an Autosizer IIc (Malvern, UK) equipped with a He–Ne laser. A Malvern K7032090 autocorrelator was used. The software provided by the manufacturer was employed to calculate D values. An average value over 10 consecutive measurements is reported.

Electrophoretic mobility (EPM) of vesicles and their complexes with polyelectrolytes was measured by laser microelectrophoresis in a thermostatic cell using a Zetasizer IIc (Malvern) equipped with a He–Ne laser. A Malvern K7032090 autocorrelator was also used. To determine EPM values, the software provided by the manufacturer was employed.

Phase transitions in DPPC/CL^{2-} SUVs were controlled by differential scanning calorimetry (DSC) technique with a DASM-4 adiabatic microcalorimeter (Institute for Biological Instrumentation of Russian Academy of Science, Russia). The samples were prepared as follows. Solutions of vesicles and PL in a 10^{-2} M phosphate buffer, pH 7, were heated separately up to 55 °C and then mixed. The mixtures obtained were kept for 5 min at 55 °C, then cooled to a room temperature and placed into a microcalorimeter measuring cell. The calorimetric curves were registered, heating the samples at a 1 °C/min rate within the range of 25–50 °C.

Fluorescence intensity of pyrene-labeled vesicle suspensions was measured using a F-4000 fluorescence spectrophotometer (Hitachi, Japan) at λ_{em}=440 nm (λ_{ex}=350 nm). The pH measurements were done using a PHM83 potentiometer with standard glass electrode 2040 C (Radiometer, Denmark).

To measure the amount of PL unbound to vesicles, PL-FITC was used. PL-FITC/vesicle complex particles were separated from a supernatant by passing suspension samples through the microcentrifuge Duarapore filters with a pore diameter of 0.22 μm (Sigma). Then, the fluorescence intensity at λ_{em}=525 nm (λ_{ex}=495 nm) in the filtrates was determined using a F4000 spectrofluorometer. The concentration of PL-FITC was calculated using the calibration curve.

Permeability of the vesicular membranes towards a simple salt was investigated by measuring a conductivity of NaCl-loaded vesicle suspensions with CDM83 conductometer (Radiometer) as described in Ref. [11].

Kinetics of transmembrane permeation of Dox, characterized by a strong fluorescence at λ_{em}=490 nm (λ_{ex}=557 nm), was investigated using the procedure described in Ref. [16]. Dox molecule contains amino group with pK_a 8.6, so in neutral or slightly alkaline solutions a part of Dox molecules is noncharged and can incorporate into the vesicular membrane. If the internal vesicle cavity is loaded with an acidic buffer, Dox desorbs from the membrane and accumulates inside liposomes, which finally results in self-quenching of Dox fluorescence. This allows to control the transmembrane Dox permeation by measuring the fluorescence intensity in the system.

According to this scheme, in the present work, EL/CL^{2-} SUVs were prepared in 0.3 M Tris–citrate buffer solution with pH 5, using the sonication procedure described above, and then passed through a Sephadex G-50 column, equilibrated with 20 mM Tris–citrate buffer with pH 7.5, additionally containing 0.3 M sucrose for osmotic pressure compensation. Suspensions of pH-gradient EL/CL^{2-} SUVs with pH 5 inside vesicles and pH 7.5 in surrounding solution were thus prepared. Hydrodynamic diameter of such vesicles, measured by photon correlation spectroscopy, was in the 80–100 nm range.

Dox was added to pH-gradient vesicle suspensions at 50 μM concentration, which corresponded to the maximum Dox fluorescence intensity. When the concentration of Dox inside vesicles exceeded 50 μM, the fluorescence intensity in the system began decreasing due to the self-quenching effect, the process following the first-order kinetics. Importantly, the rate constant, calculated from the obtained kinetic curves, was in a good agreement with that evaluated by direct measurement of Dox concentration in vesicles after their separation from external free Dox and further surfactant-induced lysis. The PL-induced acceleration of the Dox transport was quantified as a k_p/k_0 ratio, where k_p and k_0 are the rate constant values in the presence and in the absence of PL, respectively.

To prepare solutions, double-distilled water was used additionally treated by passing it through Milli-Q system (Millipore, USA) equipped with ion-exchange and adsorption columns as well as a filter to remove large particles.

3. Results and discussion

3.1. Binding of PL to negative SUVs

In Fig. 1a, the results of potentiometric (curve 1) and conductometric titration (curve 2) of a water solution of PL with HCl solution are presented. Before the titration procedures, PL hydrobromide was transformed into a free-base form by addition of an equimolar amount of NaOH. The

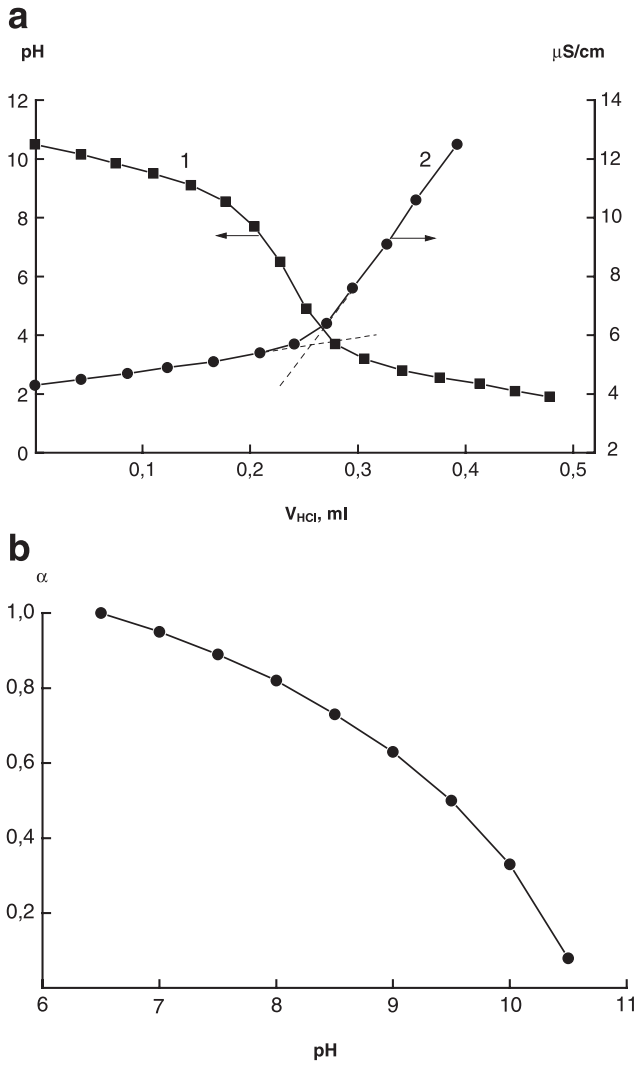

Fig. 1. (a) Potentiometric (1) and conductometric (2) titration of a PL water solution with HCl solution. [PL]=5×10^{-3} M; V_{PL}=5 ml; [HCl]=10^{-1} M. (b) Dependence of a degree of PL amino groups protonation, α, on pH value.

volume of HCl solution, required for a complete titration of NH_2 groups of PL, corresponds to an inflection of curve 2. Based on the data of potentiometric titration, a dependence of a degree of protonation of PL amino groups, α, on pH was calculated (Fig. 1b). The interaction of PL with negative vesicles was studied at pH 7, i.e. nearly maximum α value.

The starting point was to study the interaction of PL with EL/CL^{2-} SUVs (v=0.2) at 20 °C. Under these conditions, the vesicular membrane was in the fluid state [7] and lipid molecules were able to move in lateral and transmembrane directions. As shown in Ref. [17], liquid EL/CL^{2-} SUVs were characterized by nearly uniform distribution of anionic CL^{2-} molecules between both leaflets of the membrane. Adsorption of PL on negative SUVs led to neutralization of the surface charge of vesicles that was controlled by measuring their EPM value with laser microelectrophoresis techni-

que (curve 1, Fig. 2). When PL concentration increased, the EPM value decreased to zero and then became slightly positive. These findings proves adsorption of PL molecules on the surface of EL/CL^{2-} vesicles and formation of PL–lipid complexes at the water–membrane interface, stabilized by multipoint ionic contacts between the positive PL units and negative CL^{2-} headgroups. At the same time, the size of PL–vesicle complex particles continuously rose as PL concentration increased, and reached the maximum value at the PL concentration corresponding to a complete neutralization of the vesicle surface charge, i.e. at EPM=0 (cf. curves 1 and 2 in Fig. 2). Further addition of PL did not affect the complex particle size. Most likely, a slight positive charge brought by adsorbed PL was insufficient to stabilize PL–vesicle complex particles against aggregation.

Adsorption of PL on EL/CL^{2-} SUVs was also studied by measuring concentrations of FITC-labeled PL in the filtrates after passing each SUV suspension sample treated with the labeled PL through the microcentrifuge filters in the independent experiments. It was found that PL was completely bound to SUVs unless its concentration exceeded 1.8×10^{-4} M. At higher concentrations, unbound PL appeared in a solution.

The stability of PL–SUV complexes in aqueous–salt media was studied by a fluorescence technique. Cationic polymers, in particular, PL, are known to be effective fluorescence quenchers. Therefore, formation as well as dissociation of PL–SUV complexes can be followed by measuring fluorescence intensity of a labeled lipid incorporated into the membrane. Adsorption of PL on the surface of the pyrene-labeled EL/CL^{2-} SUVs was accompanied by fluorescence quenching. The ultimate level of fluorescence achieved in the system (ca. 1 min after mixing) was approximately 40% (curve 1, Fig. 3) due to quenching of fluorescence of the label in the outer membrane leaflet (see below). Further addition of NaCl to the PL–SUV suspension resulted in recovery of the fluorescence intensity up to initial level (curve 2), indicating a complete dissociation of the PL–vesicle complex due to a shielding effect of Na^+ and Cl^- ions. Such dissociation, in turn, led to a decrease of size of particles in the suspension down to the initial vesicle size. The latter positively indicated that integrity of EL/CL^{2-} SUVs retained when complexed with PL.

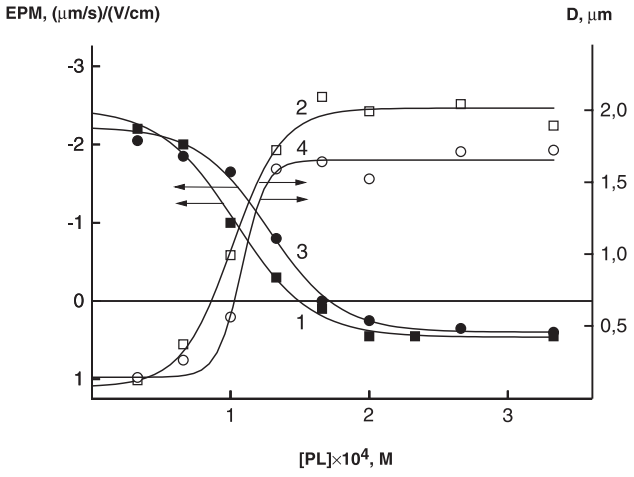

Fig. 2. Dependence of EPM (1) and size (2) for EL/CL^{2-} SUVs, and EPM (3) and size (4) for DPPC/CL^{2-}SUVs (v=0.2 for both) on PL concentration. $2[CL^{2-}]=2.8\times10^{-4}$ M; 10^{-2} M phosphate buffer, pH 7; 20 °C.

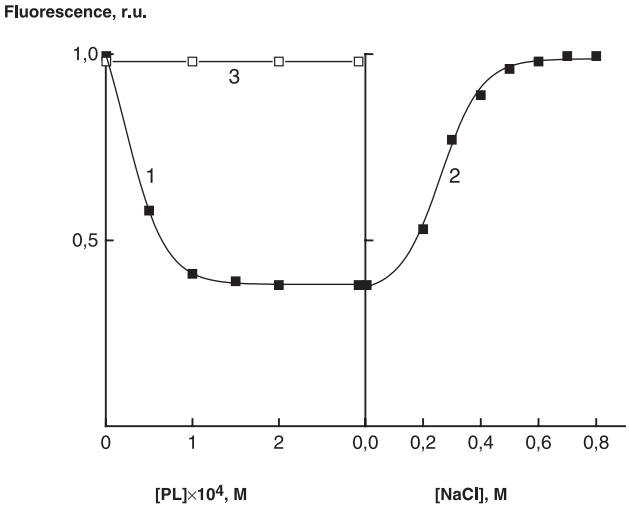

Fig. 3. Dependence of relative fluorescence intensity for pyrene-labeled EL/CL^{2-} SUVs (v=0.2) on PL concentration (1), for PL-SUV complex on NaCl concentration (2), and for PL–SUV complex in the presence of PAA (3). To obtain curve 2, PL–SUV complex was prepared at the point A and NaCl was then added at different concentrations. To obtain curve 3, PL–SUV complexes with different PL/SUV ratios were prepared and PAA was then added to the complexes at [PAA]/[PL]=3. In all experiments, $2[CL^{2-}]=2.8\times10^{-4}$ M; 10^{-2} M phosphate buffer, pH 7; 20 °C.

To estimate the content of CL^{2-} molecules, involved in ionic contacts with adsorbed PL units, γ, we applied the procedure originally described in Ref. [18]. Obviously, at the point EPM=0, the positive charge introduced by adsorbed PL was equal to the negative surface charge of EL/CL^{2-} SUVs. In other words, the concentration of positive PL units electrostatically complexed to CL^{2-} headgroups, $[PL]_c$, was equal to the concentration of CL^{2-} headgroups exposed on the outer leaflet of the vesicular membrane, $2[CL^{2-}]_{out}$. Then, the γ value could be determined as $\gamma=2[CL^{2-}]_{out}/2[CL^{2-}]_t$, which equaled an $[PL]_c/2[CL^{2-}]_t$ ratio, where $2[CL^{2-}]_t$ was the total concentration of anionic CL^{2-} headgroups in the system. The calculation, based on the data in Fig. 2, gave γ=0.52. It means that only CL^{2-} molecules from the outer leaflet of the liquid EL/CL^{2-} SUV membrane were involved in complexation with adsorbed PL.

This conclusion was confirmed in the experiments with DPPC/CL^{2-} SUVs with the same CL^{2-} headgroup content (v=0.2). The membrane of a such vesicle, in contrast to that of a EL/CL^{2-} vesicle, was not in a liquid but in the gel state at 20 °C (solid vesicles). The effect of PL on EPM and size of solid DPPC/CL^{2-} SUVs is represented by curves 3 and 4 in Fig. 2. It is seen that these curves are located close to

curves 1 and 2 in the same figure, respectively, reflecting the changes in EPM and size of liquid EL/CL^{2-} SUVs in the presence of PL. It has been shown earlier [17,18] that in solid DPPC/CL^{2-} SUVs, similar to liquid EL/CL^{2-} ones, CL^{2-} molecules are uniformly distributed between both leaflets of the vesicular membrane. However, in the solid DPPC/CL^{2-} SUVs vesicles, transmembrane migration of lipid molecules is highly restricted, and only CL^{2-} molecules from the outer membrane leaflet are able to form ionic contacts with adsorbed PL. So, the practical coincidence of curves presented in Fig. 2 proved that adsorbed PL was able to form salt bonds only with the outer CL^{2-} molecules both in liquid EL/CL^{2-} and solid DPPC/CL^{2-} vesicles.

It has been shown earlier that polycations, including PL, when adsorbed on mixed negative lipid membranes, can induce the lateral lipid segregation, i.e. formation of 2 two-dimensional microphases: one enriched with neutral lipid molecules, and the other with negative lipid molecules complexed with adsorbed polycation chains. Up to now, a number of methods for controlling lipid segregation has been developed, including electron microscopy [19,20] as well as ESR [10,20], NMR [21], Raman [22,23], infrared [22] and fluorescence [20,24] spectroscopies. In the present work, PL-induced lateral lipid segregation in mixed DPPC/CL^{2-} SUVs was observed using DSC technique as described in Refs. [13,25]. The phase transition in DPPC bilayer is characterized by a narrow peak with maximum at 41.5 °C (curve 1, Fig. 4) that is in a good agreement with the earlier reported data [26]. The other component of the vesicular membrane, CL^{2-}, actually represents a mixture of natural lipids with a set of phase transition temperatures below 10 °C [13]. The mixed DPPC/CL^{2-} SUVs revealed a wide phase transition temperature range with a maximum at 36.5 °C and a shoulder at 31.5 °C (curve 2, Fig. 4), probably reflecting the melting of the two membrane regions with different amounts of CL^{2-}. Then, increasing amounts of PL were added to the vesicle suspension. For this, the suspension of vesicles and PL solution were heated separately up to 55 °C and then mixed. In other words, PL interacted with DPPC/CL^{2-} SUVs whose membrane were preconverted to the fluid state. The mixtures obtained were kept at 55 °C for 5 min, then cooled to a room temperature and placed into the microcalorimeter measuring cell. As PL concentration in the mixed PL–vesicle suspension increased, the peak in the calorimetric curve gradually shifted to the higher temperatures and became narrower (curves 3–6). Based on the data of Refs. [10,13,19,20,22–24], it is reasonable to attribute these changes to formation of DPPC-enriched regions in the vesicular membrane due to segregation of CL^{2-} molecules, interacted with adsorbed PL chains, into separate domains.

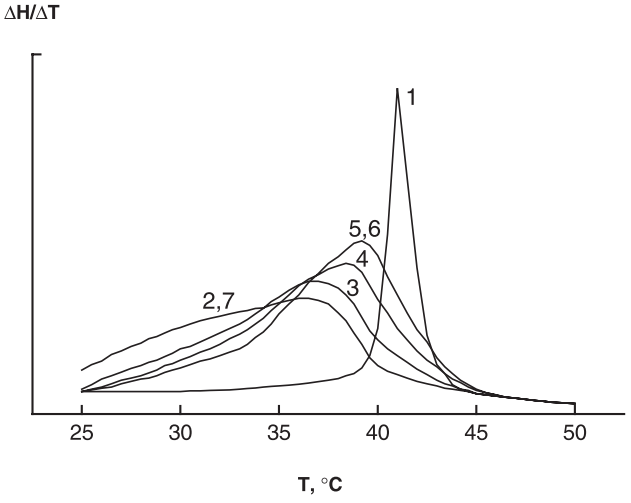

Fig. 4. Calorimetric curves for DPPC SUVs (1), DPPC/CL^{2-} SUVs and DPPC/CL^{2-} LUVs (2), complexes of DPPC/CL^{2-} SUVs with PL (3–6), and ternary PL/DPPC–CL^{2-} LUV/PAA system (7). To obtain curve 7, PAA–PL IPEC was prepared at [PAA]/[PL]=2 and then added to DPPC–CL^{2-} LUVs, characterized by the melting curve 2. v=0.2 for all vesicles; 2[CL^{2-}]=2.8×10^{-4} M; [PL]=5×10^{-5} (3), 1×10^{-4} (4), 1.5×10^{-4} (5, 7) and 2×10^{-4} M (6); 10^{-2} M phosphate buffer, pH 9.2.

An alternative explanation of the above changes might be an increase in the temperature of the gel-to-fluid phase transition of the vesicular membrane due to neutralization of CL^{2-} negative charges by adsorbed polycation. Indeed, polycation binding is able to increase the phase transition temperature up to nearly 20 °C depending on a type of negative lipid heads and molecular mass of polycation [19,24,27,28]. However, it has been shown using the DSC technique that the phase transition temperature for CL^{2-} electrostatically complexed with a polycation lies below 25 °C [13]. Therefore, the observed shift of the peak in the calorimetric curve from 36.5 °C to higher temperatures could not result simply from charge neutralization of CL^{2-} heads by adsorbed PL.

The changes in the calorimetric curves of DPPC/CL^{2-} SUVs developed unless PL concentration reached 1.5×10^{-4} M (cf. curves 5 and 6 in Fig. 4). The number of PL repeating units in the system at the above PL concentration was equal to a half of CL^{2-} molecules initially distributed in the vesicular membrane. Taking into account the initial uniform distribution of CL^{2-} molecules between the both membrane leaflets, this fact apparently shows that only the outer CL^{2-} molecules were involved in the segregation process induced by adsorbed PL.

Interestingly, the earlier-studied behavior of liquid negative vesicles in the presence of another polycation, poly(*N*-ethyl-4-vinylpyridinium bromide) (PEVP), was quite different. Indeed, binding of PEVP to liquid EL/CL^{2-} SUVs forced CL^{2-} molecules to transfer from the inner to outer leaflet of the vesicular membrane [7]. The DSC study of DPPC/CL^{2-} SUVs in the presence of PEVP showed that in this case, the changes in the calorimetric curves were observed unless polycation concentration, required for a complete neutralization of all CL^{2-} molecules from both membrane leaflets, was achieved. Importantly, the final melting peak superimposed on that of the single-component DPPC vesicles [13]. This definitely indicates that PEVP-

induced flip-flop in liquid DPPC–CL^{2-} SULs was accompanied by lateral lipid segregation, i.e. formation of CL^{2-} patches within the outer leaflet of the bilayer contacting with the adsorbed polycation. These rearrangements caused an abnormal asymmetry in charge distribution: all negative lipid molecules were concentrated on the outer leaflet of the membrane and clusterized providing a maximum amount of ionic contacts with the polycations. In contrast to this, PL electrostatically interacted only with the outer CL^{2-} molecules followed by their clusterization but did not change a distribution of lipids in the inner membrane leaflet. Therefore, the final calorimetric curve obtained in the DPPC–CL^{2-} SULs–PL system actually represents a combination of two: first describing the melting of the outer segregated leaflet and second reflecting the melting of the unaffected inner, with a peak at 39.2 °C located between the melting peaks of both components.

The mechanism of a sharp acceleration of the transmembrane lipid migration in the presence of PEVP and the reason of different responses of the vesicular membrane to PEVP and PL adsorption are still unclear. Flip-flop rearrangement is shown to proceed slowly even in bilayers of intact liquid vesicles as a result of thermal motion. We have hypothesized in Ref. [29] that adsorption of PEVP, a flexible polycation with a high linear charge density, produces additional dynamic distortions in the bilayer structure, arising from electrostatic repulsion of charged units within loops and tails formed by adsorbed polymer chain. As a result, negative lipids, coming from the inner to outer leaflet, are fixed there being bounded to polycation molecules, coming from the external solution. An adequate amount of neutral lipid molecules transfer to the inner leaflet, thus ensuring the integrity of the vesicular membrane. At the same time, it was shown that rather long PL molecules, when adsorbed on the negative lipid membrane, were able to acquire β-sheet conformation and to form rigid interfacial polymer layers, stabilized by intramolecular hydrogen bonds [12,30]. Because of strong structural restrictions, PL molecules, involved in such layers, could not form loops and tails exposed into water solution, as it was in the case of PEVP, and therefore were not able to accelerate flip-flop in excellent agreement with the experimental data.

It is loops and tails formed by adsorbed PEVP chains that obviously ensured changing vesicle charge from negative to positive and stability of vesicle–PEVP complex particles against aggregation in the excess of polycation that has been described in detail in Refs. [13,29]. In contrast to this, an extremely slight positive surface charge of the same vesicles in the excess of PL, insufficient to stabilize PL–vesicle complex particles, apparently resulted from rigid β-sheet conformation of adsorbed PL macromolecules.

3.2. Binding of PL to LUVs

In contrast to rigid SUVs, which are difficult to change shape, regular cells are characterized by a rather high ductility, allowing them to withstand considerable deformations without destruction. The cell size is usually in the micron region, i.e. 2 orders of magnitude higher than that of the above studied SUVs. One may expect that increase in the vesicular size at fixed lipid composition would provide a better model to mimic cell interaction with polycationic species. Therefore, we examined interaction of PL with EL/CL^{2-} LUVs of ν=0.2 as the next step.

At first sight, such interaction followed the same regularities as described above for the mixture of PL with EL/CL^{2-} SUVs of the same lipid composition. Indeed, PL adsorption was accompanied by neutralization of the vesicle surface charge (curve 1, Fig. 5), enlargement of suspension particles (curve 2), and quenching of the fluorescence of pyrene-PC incorporated into the membrane (curve 1, Fig. 6). Lastly, only CL^{2-} molecules located in the outer LUV membrane leaflet formed ionic bonds with adsorbed PL units: γ value, calculated from the data of Fig. 6, was close to 0.5.

However, the behavior of the complexes formed by PL with small and large pyrene-labeled EL/CL^{2-} vesicles in water salt solutions was quite different. As mentioned above, in the case of labeled EL/CL^{2-} SUVs, the fluorescence, partially quenched by complexed PL (curve 2, Fig. 3), as well as the particle size, was recovered up to initial level on addition of 0.4 M NaCl solution. In contrast, the addition of NaCl solution to the complex of PL with labeled EL/CL^{2-} LUV suspension had no effect on the fluorescence intensity up to [NaCl]=1 M (curve 2, Fig. 6). It means that PL was not removed from the surface of LUVs that was in the line with only slight recovery of the complex particle size on adding NaCl (data not shown).

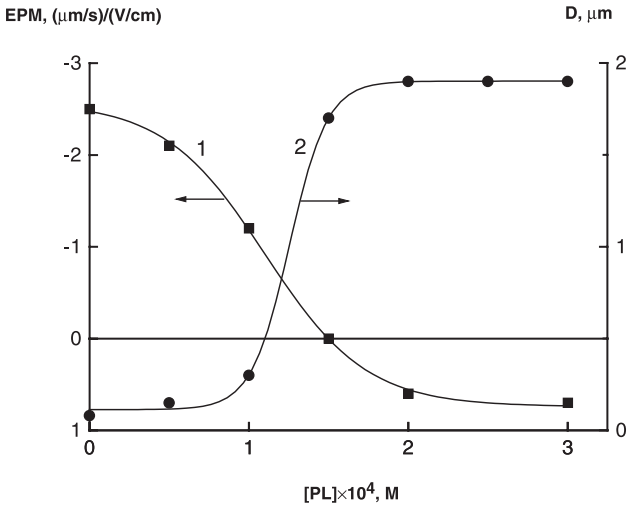

Fig. 5. Dependence of EPM (1) and size (2) for EL/CL^{2-} LUVs (ν=0.2) on PL concentration. 2[CL^{2-}]=2.8×10^{-4} M; 10^{-2} M phosphate buffer, pH 7; 20 °C.

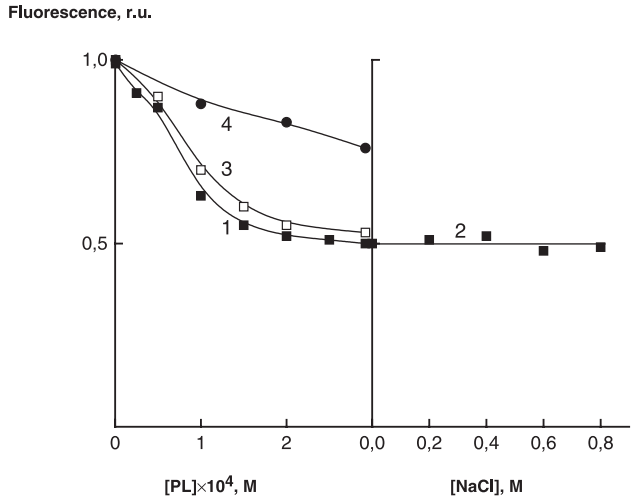

Fig. 6. Dependence of relative fluorescence intensity for pyrene-labeled EL/CL^{2-} LUVs on PL concentration (1), for PL–LUV complex on NaCl concentration (2), and for PL–LUV complex in the presence of PAA (3, 4). To obtained curve 2, PL–LUV complex was prepared and PAA was then added at [PAA]/[PL]=3. To obtain curve 3, PL–LUV complexes with different PL/LUV ratios were prepared and PAA was then added to the complexes at [PAA]/[PL]=3. To obtain curve 4, PAA–PL (3:1) IPEC was prepared and added to LUVs. v=0.2 for all vesicles; 2[CL^{2-}]=2.8×10^{-4} M; 10^{-2} M phosphate buffer, pH 7; 20 °C.

3.3. Competitive reactions in the vesicle–PL–PAA ternary system

It is known that oppositely charged linear polyelectrolytes form interpolyelectrolyte complexes (IPECs) in aqueous solutions [6,31–33]. Therefore, in the ternary system containing negative vesicles, PL and PAA, one should expect a competition of vesicles and PAA for binding to PL.

Addition of PL solution to PAA solution (in the absence of vesicles) resulted in neutralization of charges of both polyelectrolytes. Zero EPM value was observed at the stoichiometric ratio of the components, i.e. at [PAA]/[PL]=1, which is evidence of their quantitative binding to each other to form a strong IPEC.

A competition in the ternary system was studied as described in Refs. [13,29,34]. Briefly, complexes containing pyrene-labeled EL/CL^{2-} vesicles and various amount of PL were prepared and equilibrated. Then, PAA was added to each sample of PL–vesicle complexes so that [PAA]/[PL] ratio was equal to 3. Possible removal of PL from the vesicle surface due to recomplexation with PAA could be detected by increase in pyrene fluorescence intensity.

As follows from the data of Fig. 3 (curve 3), addition of PAA to the complexes of PL with labeled EL/CL^{2-} SUVs resulted in recovery of pyrene fluorescence intensity up to the initial level. Correspondingly, the size of PL–SUV complex particles decreased down to that of the initial EL/CL^{2-} SUVs. This indicates a complete removal of PL from the membrane of EL/CL^{2-} SUVs due to recomplexation and formation of water-soluble PAA–PL IPEC.

In contrast to that, addition of PAA to the complexes of PL with labeled EL/CL^{2-} LUVs led only to a negligible increase in pyrene fluorescence intensity (curve 3, Fig. 6) and had only a slight effect on the size of PL–vesicle complex particles. It means that PAA could not remove PL from the surface of EL/CL^{2-} SUVs. At the same time, addition of a three-fold excess of FITC-labeled PAA to the complex of PL with unlabeled LUVs was accompanied by a partial decrease in the PAA fluorescence intensity. It means that PAA–PL IPEC was formed in this case as well. However, it retained contacting the vesicle surface probably due to incorporation of PL pendant groups and/or short fragments of backbone PL into the lipid membrane. In other words, an excess of the polyanion could not decompose already-formed complex of PL with large liquid negative vesicles.

It is known that biological liquids contain high amounts of negative multicharged species (proteins, polysaccharides) whose mobility considerably exceeds that of cells. Therefore, it should be expected that polycations, introduced to a biological liquid, will first bind to such species. In this connection, an important problem arises: Will polycations be able to interact with cells, being already bound to an excess of a competing negatively charged component?

To examine this problem, negative PAA–PL IPEC was prepared and added to the suspension of pyrene-labeled EL/CL^{2-} LUVs. This led to a decrease of fluorescence intensity in the system (curve 4, Fig. 6). The observed effect could result from adsorption of either the whole PAA–PL IPEC or only its cationic component, i.e. PL, on the vesicle surface. To clarify whether the PAA–PL complex dissociated, when contacted the vesicle surface, or not, the complex of fluorescently labeled PAA and PL of the same composition was prepared and then added to nonlabeled EL/CL^{2-} LUVs. It was found that PAA fluorescence, originally quenched in PAA–PL IPEC, was not recovered. It proves that PAA–PL complex interacted with EL/CL^{2-} SUVs without dissociation, and adsorbed on the vesicular surface as a whole.

The behavior of a system, containing negative LUVs and negative PAA–PL IPEC, was also examined with the microcalorimetric technique. For this, DPPC/CL^{2-} LUVs with v=0.2 were used. The phase transition in the bilayer of such vesicles, both small and large, is described by curve 2 in Fig. 4. Curve 7 in the same figure, coinciding with curve 2, corresponds to melting of DPPC/CL^{2-} LUVs after addition of negative PAA–PL IPEC to the LUV suspension. It means that PL did not form ionic contacts with CL^{2-} molecules, thus supporting the above conclusion that there was no dissociation of PAA–PL IPEC in the presence of DPPC/CL^{2-} LUVs. Negative PAA–PL IPEC likely bound to DPPC/CL^{2-} LUVs due to incorporation of its domains formed by mutually neutralized PAA and PL units into the hydrophobic part of the vesicular membrane.

3.4. Modulation of permeability of negative vesicular membrane by interaction with PL

Two different paths for species to penetrate through the vesicular membrane are commonly discussed in the literature [35,36]. The first relates to formation of transient pores or other membrane defects permeable for small inorganic and organic ions (channel mechanism). The second consists of two steps: partition of species into the hydrophobic part of the membrane followed by their diffusion into the vesicle water cavity (partition–diffusion mechanism). The latter mechanism is mainly responsible for the penetration of noncharged molecules.

A possible effect of PL on the permeability of the membrane towards small ions was investigated by a conductivity approach using a suspension of lipid vesicles loaded with concentrated NaCl solutions [8]. Conductivity of the initial NaCl-loaded EL/CL^{2-} SUVs with v=0.2 did not change within at least 1 h. Addition of PL to the NaCl-loaded vesicles also had no effect on the suspension conductivity during the same period of time, indicating that PL did not induce formation of transient defects in the lipid membrane.

In contrast to EL/CL^{2-} SUVs, addition of PL to suspension of NaCl-loaded EL/CL^{2-} LUVs with the same CL^{2-} content was accompanied by a 95% increase in the suspension conductivity for the time of mixing of the components (a few seconds). Similar effect was observed when NaCl-loaded EL/CL^{2-} LUVs were mixed with a negative PAA–PL (2:1) IPEC: the salt was completely released from the vesicles 30 s after mixing. Such a sharp rise of the membrane permeability towards small ions was probably due to incorporation of PL and IPEC fragments into the vesicular membrane, resulting in the formation of transient pores and/or some other defects in it.

To study the permeability of lipid membranes towards noncharged molecules according to the partition–diffusion mechanism, Dox was added to suspensions of pH-gradient EL/CL^{2-} vesicles with pH 5 inside and pH 7.5 in the surrounding solution. Only negative SUVs were used in these experiments because their membranes, in contrast to those of negative LUVs, remained impermeable towards a simple salt, i.e. retained their integrity, in the presence of PL. As mentioned above, Dox molecule contains an amino group with pK_a 8.6, so at pH 7.5, about 5% of Dox molecules in solution are noncharged and can incorporate into the vesicular membrane. Their desorption inside vesicles, followed by protonation of Dox molecules, is accompanied by self-quenching of Dox fluorescence. This process, following the first-order kinetics, reflected the transmembrane Dox permeation.

Kinetics of Dox permeation through the membrane of pH-gradient EL/CL^{2-} SUVs is described by curve 1 in Fig. 7a. Curve 2 in the same figure describes a typical kinetics of Dox permeation in the presence of PL. The addition of the latter, being an effective fluorescence quencher, was accompanied by some decrease both in initial and final levels of Dox fluorescence intensity. The decrease could also result from aggregation of vesicles contacting with PL and increase in suspension turbidity. By analyzing the kinetic curves for different concentrations of PL, the rate constants of Dox permeation were quantified. The effect of PL on Dox permeation is represented in Fig. 7b as a k_p/k_0–$Z_{+/-}$ plot, where k_p and k_0 are the rate constants in the presence and in the absence of PL, respectively, and $Z_{+/-}$=$[PL]_c/[CL^{2-}]_t$ is equal to the ratio between the number of positive PL units bound to EL/CL^{2-} SUVs and the total number of CL^{2-} headgroups in the system. One can see that the effect of PL increases upon $Z_{+/-}$ increase, reaching the maximum k_p/k_0 value at $Z_{+/-}$=0.5, i.e. at a complete neutralization of the

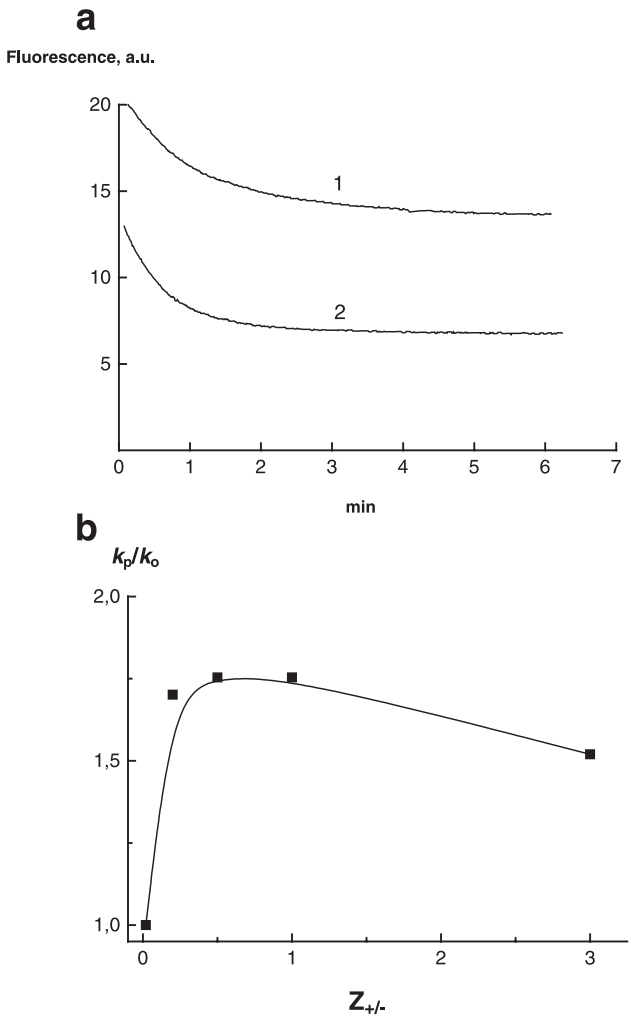

Fig. 7. (a) Kinetics of Dox permeation through the membrane of pH-gradient EL/CL^{2-} SUVs (v=0.25) in the absence (1) and in the presence of PL (2). 2[CL^{2-}]=3.3×10^{-4} M; [PL]=1.7×10^{-4} M; external buffer: 20 mM Tris–citrate, pH 7.5, supplied with 0.3 M of sucrose; internal buffer: 0.3 M citrate–Tris pH 5.0; 25 °C. (b) Dependence of PL-mediated Dox permeation through the membrane of pH-gradient EL/CL^{2-} SUVs (v=0.25) at $Z_{+/-}$ value. 2[CL^{2-}]=3.3×10^{-4} M; [PL]=1.7×10^{-4} M; external buffer: 20 mM Tris–citrate, pH 7.5, supplied with 0.3 M of sucrose; internal buffer: 0.3 M citrate–Tris pH 5.0; 25 °C.

vesicle surface charge by adsorbed PL, as shown by microelectrophoresis measurements.

A possible effect of the surface charge of EL/CL^{2-} SUVs on the kinetics of the transmembrane Dox permeation, both PL-free and PL-mediated, was also examined. For this, pH-gradient SUVs with a different molar content of negative CL^{2-} headgroups (v) were used. PL was added to vesicle suspensions so that $Z_{+/-}$=0.5. The results given in Fig. 8 show that an increase in v had opposite effects on k_0 and k_p values: the former decreased (curve 1) while the latter increased (curve 2). The reduction in k_0 with increase in the content of anionic lipid in the membrane was in agreement with the earlier-reported data [37]. It was likely due to a strong binding of positive Dox molecules in the outer leaflet of negative vesicular membrane. Such a binding obviously shifted an equilibrium

$$NH_2(Dox) + H^+ \leftrightarrow NH_3^+(Dox) \quad (1)$$

to the protonated form of Dox, thus decreasing concentration of the noncharged form and decelerating its transmembrane permeation. Addition of cationic PL to the suspension of pH-gradient EL/CL^{2-} SUVs, covered with protonated Dox, was accompanied by the formation of a strong PL–CL^{2-} interfacial complex and release of positive Dox molecules from the vesicle surface to the solution. This, in turn, led to the increase in concentration of noncharged Dox according to equilibrium 1 and the consecutive rise of k_p value. Another possible reason for increase in k_p was related to the above-described PL-induced lateral lipid segregation in the membrane and formation of patches composed of CL^{2-} species neutralized by bound PL chains. Such patches and/or boundaries between them and surrounding lipid bilayer could be responsible for acceleration of transmembrane Dox permeation as it has been hypothesized in Ref. [38].

Table 1
Effect of PL and PEVP on the permeation of Dox through the membrane of EL/CL^{2-} SUVs

Polycation	v	k_p/k_0
PL	0.1	1.05
	0.2	1.35
PEVP	0.1	1.2
	0.2	2.8

The overall effect of the v value on the PL-mediated Dox permeation, expressed as k_p/k_0 ratio, is described by curve 3 in Fig. 8. It is seen that increase in v from 0 to 0.3 resulted in nearly 2.5-fold rise in the effect of PL on transmembrane Dox permeation. Recently, the permeation of Dox through the membrane of EL/CL^{2-} SUVs in the presence of another polycation, PEVP, has been examined [38]. The maximum PEVP effect was also observed at a complete neutralization of the surface vesicle charge by the adsorbed polycation, but approached at $Z_{+/-}$=1 because of PEVP-induced migration of anionic CL^{2-} molecules from the inner to the outer leaflet of the vesicular membrane, which does not occur in the case of PL. The effect of both polycations, PL at $Z_{+/-}$=0.5 and PEVP at $Z_{+/-}$=1, on the Dox permeation is shown in Table 1.

As the table shows, PEVP demonstrates more pronounced effect on Dox permeation. Since the k_0-v dependence is obviously the same for both polycations, it means that the rate constant for Dox permeation in the presence of PEVP is higher than in the case of PL. The integrity of the

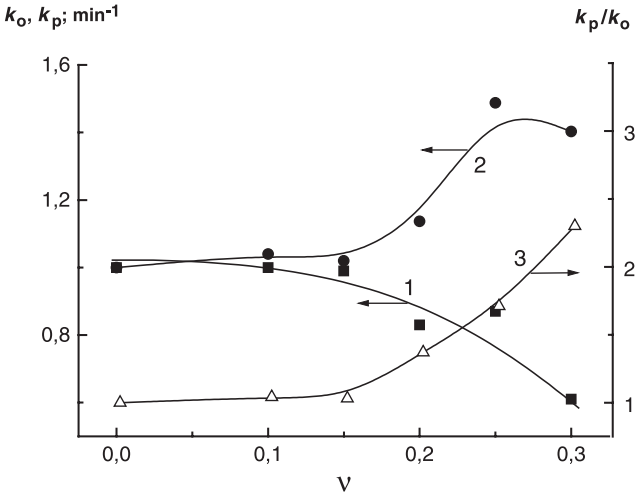

Fig. 8. Dependence of k_0 (1), k_p (2) and k_p/k_0 ratio (3) for Dox permeation through the membrane of pH-gradient EL/CL^{2-} SUVs on v value. PL was added to SUVs at $Z_{+/-}$=0.5. External buffer: 20 mM Tris–citrate, pH 7.5, supplied with 0.3 M of sucrose; internal buffer: 0.3 M citrate–Tris pH5.0; 25 °C.

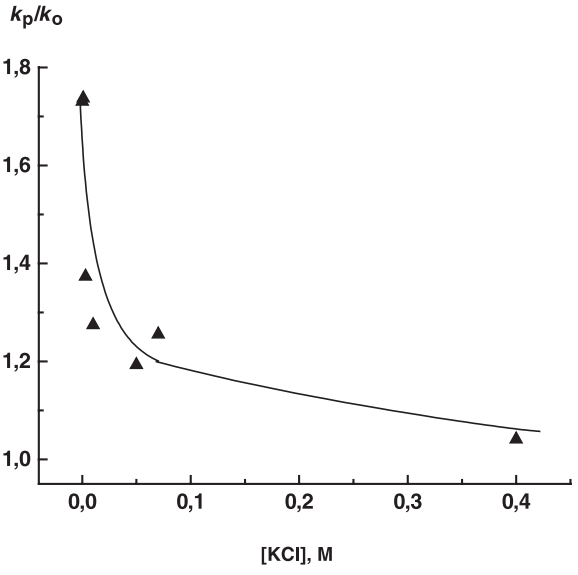

Fig. 9. Dependence of PL-mediated Dox permeation through the membrane of pH-gradient EL/CL^{2-} SUVs (v=0.2) on KCl concentration. 2[CL^{2-}]=2.6×10^{-4} M; [PL]=1.3×10^{-4} M; external buffer: 20 mM Tris–citrate, pH 7.5, supplied with 0.3 M of sucrose; internal buffer: 0.3 M citrate–Tris pH 5.0; 25 °C.

membrane of EL/CL^{2-} SUVs ($v \leq 0.3$) complexed with PEVP has been shown to be unchanged [8], indicating that PEVP-induced flip-flop of CL^{2-} molecules is accompanied by migration of adequate amounts of neutral EL molecules to the opposite direction, i.e. from the outer to the inner membrane leaflet. Therefore, at EPM=0 point, the inner leaflet becomes electrically neutral and does not obstruct desorption of protonated Dox molecules inside the vesicles. In the present work, it is found that PL interacts only with the outer CL^{2-} molecules of EL/CL^{2-} SUVs, neutralizing their charges. So, the inner membrane leaflet retains the negative charge and can electrostatically bind Dox molecules that are protonated after their translocation through the vesicular membrane. Such binding apparently decelerates desorption of Dox from the inner membrane leaflet and finally resulted in decrease in k_p and k_p/k_0 values.

By increasing the concentration of a simple salt in the surrounding solution, the PL effect on Dox permeation through the membrane of liquid EL/CL^{2-} SUVs could be completely but reversibly suppressed (Fig. 9), apparently because of the desorption of PL molecules from the vesicular membrane.

4. Conclusions

When interacting with liquid EL/CL^{2-} SUVs and LUVs, cationic PL neutralizes CL^{2-} molecules originally located on the outer leaflet of the vesicular membrane, i.e. at $Z_{+/-} = 0.5$. The interaction is accompanied by the formation of 2 two-dimensional microphases: one composed of CL^{2-} molecules electrostatically tied with adsorbed PL units and another composed of neutral EL molecules. The process develops only on the outer membrane leaflet. The binding of PL to SUVs is reversible: PL can be removed from the vesicle surface by increase in ionic strength of the solution or by recomplexation with a polyanion. PL binding does not affect ionic permeability of the EL/CL^{2-} SUV membrane but increase permeability towards noncharged Dox molecules, the maximum effect being observed at $Z_{+/-} = 0.5$. The permeabilizing PL effect grows up when increasing the CL^{2-} content in the vesicular membrane. In contrast, PL binding to EL/CL^{2-} LUVs is irreversible, probably due to the incorporation of PL fragments into a ductile membrane of the large vesicles. Such interaction is accompanied by a sharp increase in ionic permeability of the membrane.

Acknowledgements

The authors are thankful to the Russian Foundation for Fundamental Research (RFFR), Grant 02-03-33185; the US Civilian Research and Development Foundation for the Independent States of the Former Soviet Union (CRDF), Award RC1-2054; and the Fogarty International Research Cooperative Award (FIRCA), Grant TW05555, for financial support.

References

[1] R.E. Hancock, Trends Microbiol. 5 (1997) 37–42.
[2] J.P. Behr, C.R. Seances, Soc. Biol. Fil. 190 (1996) 33–38.
[3] A.S. Sobolev, A.A. Rosenkranz, O.A. Smirnova, V.A. Nikitin, G.L. Neugodova, B.S. Naroditsky, I.N. Shilov, I.N. Shatski, L.K. Ernst, J. Biol. Chem. 273 (1998) 7928–7933.
[4] A.A. Rosenkranz, S.V. Yachmenev, D.A. Jans, N.V. Serebryakova, V.I. Murav'ev, R. Peters, A.S. Sobolev, Exp. Cell Res. 199 (1992) 323–329.
[5] P. Lemieux, S.V. Vinogradov, C.L. Gebhart, N. Guerin, G. Paradis, H.K. Nguyen, B. Ochietti, Y.G. Suzdaltseva, E.V. Bartakova, T.K. Bronich, Y. St-Pierre, V.Y. Alakhov, A.V. Kabanov, J. Drug Target. 8 (2000) 91–105.
[6] V.A. Kabanov, A.V. Kabanov, Adv. Drug Deliv. Rev. 30 (1998) 49–60.
[7] A.A. Yaroslavov, V.Ye. Koulkov, A.S. Polynsky, B.A. Baibakov, V.A. Kabanov, FEBS Lett. 340 (1994) 121–123.
[8] A.A. Yaroslavov, E.A. Kiseliova, O.Yu. Udalykh, V.A. Kabanov, Langmuir 14 (1998) 5160–5163.
[9] O.M. Zakharova, A.A. Rosenkranz, A.S. Sobolev, Biochim. Biophys. Acta 1236 (1995) 177–184.
[10] H.-J. Galla, E. Sackmann, Biochim. Biophys. Acta 401 (1975) 509–529.
[11] A.E. Gad, M. Bental, G. Elyashiv, H. Weinberg, Biochemistry 24 (1985) 6277–6282.
[12] K. Fukushima, T. Sakamoto, J. Tsuji, K. Kondo, R. Shimozawa, Biochim. Biophys. Acta 1191 (1994) 133–140.
[13] A.A. Yaroslavov, A.A. Efimova, V.I. Lobyshev, V.A. Kabanov, Biochim. Biophys. Acta 1560 (2002) 14–24.
[14] H.G. Khorana, Chem. Rev. 53 (1953) 145–168.
[15] R.R.C. New, in: R.R.C. New (Ed.), Liposomes: A Practical Approach, Oxford Univ. Press, Oxford, 1990, p. 301.
[16] P.R. Harrigan, K.F. Wong, T.E. Redelmeier, J.J. Wheeler, P.R. Cullis, Biochim. Biophys. Acta 1149 (1993) 329–338.
[17] A.A. Yaroslavov, O.E. Kuchenkova, E.G. Yaroslavova, V.A. Kabanov, Dokl. Phys. Chem. 354 (1997) 350–352.
[18] A.A. Yaroslavov, A.A. Efimova, V.Ye. Kul'kov, V.A. Kabanov, Polym. Sci. 36 (1994) 215–220.
[19] W. Hartmann, H.-J. Galla, E. Sackmann, FEBS Lett. 78 (1977) 169–172.
[20] W. Hartmann, H.-J. Galla, Biochim. Biophys. Acta 509 (1978) 474–490.
[21] P.M. Macdonald, K.J. Crowell, C.M. Franzin, P. Mitrakos, D.J. Semchyschyn, Solid State Nucl. Magn. Reson. 16 (2000) 21–36.
[22] D. Carrier, M. Pezolet, Biochemistry 25 (1986) 4167–4174.
[23] G. Laroche, D. Carrer, M. Pezolet, Biochemistry 27 (1988) 6220–6228.
[24] D. Carrier, J. Dufourcq, J.-F. Faucin, M. Pezolet, Biochim. Biophys. Acta 820 (1985) 131–139.
[25] T. Ikeda, H. Yamaguchi, S. Tazuke, Biochim. Biophys. Acta 1026 (1990) 105–112.
[26] D. Bach, in: D. Chapman (Ed.), Biomembrane Structure and Function, Verlag Chemie, Basel, 1984, pp. 1–141.
[27] D. Carrer, M. Pezolet, Biophys. J. 46 (1984) 497–506.
[28] G. Laroche, M. Pezolet, J. Dufourcq, E.L. Dufourc, Prog. Colloid & Polym. Sci. 79 (1989) 38–42.
[29] A.A. Yaroslavov, E.G. Yaroslavova, A.A. Rakhnyanskaya, F.M. Menger, V.A. Kabanov, Colloids Surf., B 16 (1999) 29–43.
[30] G. Laroche, E.L. Dufourc, M. Pezolet, J. Dufourcq, Biochemistry 29 (1990) 6460–6465.
[31] E. Tsuchida, K. Abe, in: A.D. Wilson, H.J. Prosser (Eds.), Developments in Ionic Polymers, Elsevier, Amsterdam, 1986, pp. 191–267. Chapter 5.

[32] B. Philip, H. Dautzenberg, K.-J. Linow, J. Kotz, W. Dawydoff, Prog. Polym. Sci. 14 (1989) 91–172.
[33] V.A. Kabanov, A.V. Kabanov, Macromol. Symp. 98 (1995) 601–613.
[34] A.A. Yaroslavov, S.A. Sukhishvili, O.L. Obolsky, E.G. Yaroslavova, A.V. Kabanov, V.A. Kabanov, FEBS Lett. 384 (1996) 177–180.
[35] D.V. Deamer, A.G. Volkov, in: E.A. Disalvo, S.A. Simon (Eds.), Permeability and Stability of Lipid Bilayers, CRC Press, Boca Raton, FL, 1995, pp. 161–177.
[36] S. Paula, A.G. Volkov, A.N. van Hoek, T.H. Haines, A.W. Deamer, Biophys. J. 70 (1996) 339–348.
[37] G. Speelmans, R.W.H.M. Staffhorst, B. de Kruijff, F.A. de Wolf, Biochemistry 33 (1994) 13761–13768.
[38] N.O. Kozlova, I.B. Bruskovskaya, N.S. Melik-Nubarov, A.A. Yaroslavov, V.A. Kabanov, F.M. Menger, Biochim. Biophys. Acta 1514 (2001) 139–151.